Published in final edited form as:
Annu Rev Biophys. 2012 ; 41: 157–177. doi:10.1146/annurev-biophys-101211-113227.

Bacterial Mechanosensitive Channels—MscS: Evolution's Solution to Creating Sensitivity in Function

James H. Naismith[1] and **Ian R. Booth**[2]

[1]Professor Chemical Biology, Biomedical Sciences Research Complex, The North Haugh, The University, St Andrews, Fife KY16 9ST, United Kingdom; naismith@stand.ac.uk [2]Professor Emeritus Microbiology, University of Aberdeen, Institute of Medical Sciences, Foresterhill, Aberdeen, AB25 2ZD, United Kingdom; i.r.booth@abdn.ac.uk

Abstract

The discovery of mechanosensing channels has changed our understanding of bacterial physiology. The mechanosensitive channel of small conductance (MscS) is perhaps the most intensively studied of these channels. MscS has at least two states: closed, which does not allow solutes to exit the cytoplasm, and open, which allows rapid efflux of solvent and solutes. The ability to appropriately open or close the channel (gating) is critical to bacterial survival. We briefly review the science that led to the isolation and identification of MscS. We concentrate on the structure-function relationship of the channel, in particular the structural and biochemical approaches to understanding channel gating. We highlight the troubling discrepancies between the various models developed to understand MscS gating.

Keywords

protein structure; modeling; crystallography; EPR; mutagenesis; ion channel

HISTORICAL PERSPECTIVE

Bacterial Channels: An Unexpected Discovery

The discovery and analysis of mechanosensitive (MS) channels in bacteria have provoked one of the most radical changes in thinking on bacterial physiology. Prior to the discovery of MS channels, it was a widely held view that the ion impermeability of the cell membrane was a fundamental parameter critical to energy transduction and ionic homeostasis. A major breach of that barrier would, it was felt, comprise such a fundamental impairment of cell physiology that the evolution of nonspecific channels in the cytoplasmic membrane would not have occurred. We now know that such channels are ubiquitous and that they are also found in diverse compartments in plants and fungi (24, 47). Most bacteria possess multiple channel homologs in their genome. Escherichia coli has seven functionally independent MS channels that have overlapping functions (47). How the cell regulates the opening of the channels and how structure fits function are two hotly debated questions. Here we review the probable answers to these questions for the mechanosensitive channels of small (MscS) and mini (MscM) conductance families of MS channels.

The authors are not aware of any affiliations, memberships, funding, or financial holdings that might be perceived as affecting the objectivity of this review.

Europe PMC Funders Author Manuscripts

Britten & McClure (17) provided the first intimations of osmotically sensitive solute efflux pathways in a critical analysis of the factors controlling the amino acid pool formation in E. coli. They observed that washing cells with a buffer whose osmolarity is threefold lower than that of the growth medium led to more than a 75% loss of the amino acid pool. Their speculation that water inflow into the cell resulted in “consequent stretching of structure leading to increased permeability to the solute allowing a faster rate of loss of solute molecules” was remarkably prescient as a description of the modus vivendi of MS channels (Figure 1a). The lack of suitable methods to follow up this critical observation meant that the discovery of the channels themselves would not take place for another 25 years (36).

A New Passage: The First Channels Are Identified

Authentication of mechanosensing by bacterial channels required the application of two techniques: patch clamping, which allowed the recording of current passing through channels in isolated patches of membrane (23), and giant spheroplasts derived from E. coli cells that allowed patch clamping to be applied to bacteria (21, 51). By applying these technologies, Kung and colleagues (36) demonstrated stepwise increases in current, consistent with channel openings and closures, in response to small increments in imposed transmembrane pressure. The channels remained open for several milliseconds and closed when pressure was released. Initial doubts about the location of these channels (inner membrane versus outer membrane) were rapidly dispelled by their analysis in gram-positive bacteria, where a single boundary membrane exists (62, 63, 73). Kung’s observations, most probably a combination of the subsequently characterized MscS and MscK (potassium-dependent mechanosensitive channel) channels (32), and the identification of the structural gene for MscL (the mechanosensitive channel of large conductance) (60), changed the landscape for the analysis of channel behavior in bacterial cells and paved the way for detailed analysis of the structure and mechanism of gating.

The presence of at least two distinct classes of MS channels in E. coli was definitively proved by the classic biochemical approaches (61). This pivotal study involved the fractionation of membrane proteins after their detergent-based solubilization, followed by reconstitution and patch clamping on preparations derived from each fraction. Two channel activities, MscL and MscS, were defined by this study, complementing an earlier series of observations with membrane fusion that indicated the presence of multiple channels (12). Extension of the classification system led to the idea of three classes of channels: MscL, MscS, and MscM (mini), with the last having the lowest conductance (12, 43). Genes that encode MscL and MscS were identified by classical biochemical and genetic approaches supported by the availability of early genomic data (32, 60). The availability of multiple complete genomes then revealed the widespread distribution of these channels and the multiplicity of MscS homologs within single organisms (47). Structured mutant construction and separate expression of all six MscS homologs have revealed that the simple breakdown into MscS and MscM is a considerable oversimplification (M.D. Edwards, S.S. Black, S. Miller & I.R. Booth, unpublished observations).

Channel Properties

Identification of the structural genes for MscL and MscS led to confirmation of the principal function of the MS channels in bacterial cells (32) (Figure 1a). Calculations showed that small changes in the osmolarity of a bathing solute (as little as 20 mM) generate transmembrane pressure differences sufficient to lyse membranes (28). These changes are in the same range as those shown to activate MS channels in membrane patches, but the presence of the cell wall in the bacterial cell significantly changes the pressure differential required to gate channels (28, 32, 36). Creation of single mutants lacking either MscL or MscS was without immediate phenotype when challenged with a rapid decrease in external

osmolarity (downshock) (32, 60). However, a double mutant lacking both MscS and MscL lysed when the external osmolarity was decreased substantially (32). The downshock required to cause lysis in mutant cells was similar to that at which MS channels gated in parental cells sufficiently to cause acid-induced cell death during downshock (32). Restoration of either MscS or MscL on multicopy plasmids protected cells against downshock (8, 32). Thus, the principal function of the major MS channels (MscL and MscS) was defined in terms of maintenance of cell integrity during sudden osmotic transitions. When cells are transferred from high osmolarity media to low osmolarity media, the rapid inrush of water down the osmotic gradient creates a transient transmembrane pressure of 10–15 atm (16). Opening of MS channels allows the nonspecific release of solutes, which diminishes the transmembrane pressure and maintains cell wall integrity (Figure 1a). Other, more complex channel functions, particularly for the minor MS channels, might lie beneath this superficial analysis (15).

At the normal physiological levels either MscS or MscL is sufficient to protect E. coli cells from downshock damage (32, 60). However, in a mutant strain lacking all six MscS homologs and MscL (7), separate overexpression of any of the homologs from controlled promoters also can protect efficiently (M.D. Edwards, S.S. Black, S. Miller & I.R. Booth, unpublished observations). Thus, for most of the homologs their apparent lack of a role in protection against downshock is a function of the level of their expression, not any intrinsic lack of mechanosensitivity or conductance (M.D. Edwards, S.S. Black, S. Miller & I.R. Booth, unpublished observations). Mutants lacking either MscK or YbdG, in addition to loss of MscS and MscL, exhibit modified thresholds at which cell lysis occurs in response to osmotic downshock, suggesting that these channels may contribute more subtly to protection (53). Parallel observations of MscS homolog function in chloroplasts suggest the homologs aid in normal organelle development, including growth and division (24, 39). Here elimination of the channels causes defects in shape and division of these wall-less organelles. Preliminary data place some of the homologs in the immediate molecular environment of organelle division proteins (FtsZ) (71). Chloroplasts are likely to generate small osmotic gradients during photosynthesis that might be prevented from damaging chloroplast membranes by activation of the MscS homologs. Similarly, minor MS channels have the potential to allow bacterial cells to detect and repair small lesions in peptidoglycan, but definitive evidence for this is lacking.

The essential function of MS channels is the rapid passage of solutes out of the cell down their osmotic gradient. Thus, the major consequence of their activation is the creation of large transient pores in the membrane. In the presence of sustained pressure (as in membrane patches), channel closures are spontaneous events. In cells, where the channels function to relieve the pressure differential that leads to their activation, the MS channels may close more rapidly as a result of the decrease in bilayer tension that is a consequence of their activity. In addition, MscS may undergo spontaneous inactivation that is distinct from the reversible closure of the channel (32, 36). Sieving experiments estimate that the pore diameter of MscL is ~30 Å (18). Similar direct measurements have not been completed for the MscS family, but on the basis of conductance values the diameters are estimated to range from ~6–7 Å (0.1 nS; YnaI) to 14–16 Å (1 nS; MscS) (58).

For the membrane to remain essentially impermeable to protons (but not necessarily water, for which the membrane exhibits a high permeability), the closed state of the pore should have a negligible diameter. Thus, large protein rearrangements are required to bring about the reversible formation of these large pores. Sukharev (58) has estimated that an expansion of 84 Å 2 of the surface area occupied by the protein would accompany the creation of the open pore. How can this be achieved?

FIRST STRUCTURAL STUDIES

MscS Structure: A Closed Book?

MscS is the archetypal member of its family (32, 47) (Figure 1b). The protein was predicted from simple bioinformatic analyses to have three transmembrane helices (TM1–TM3), the third of which is amphipathic in its C-terminal region (32). MscS belongs to a large family of proteins with considerable variation in size, but the TM3 region is always the region of highest sequence similarity (32, 47, 64) (Figure 1b,c). The principal divergences in protein size arise from the possession of additional transmembrane domains N-terminal to the core channel domain and the possession by some members of substantial periplasmic domains (32) (Figure 1b). Prior to the crystal structure being solved, cross-linking experiments suggested a hexamer for MscS (58). However, more refined analysis, using cysteine-specific cross-linkers and a Ser267Cys mutant of E. coli MscS, confirmed that the channel is heptameric (37).

The crystal structure of MscS (9) at 3.95 Å resolution has transformed our understanding of the protein (Figure 2a). The structure showed seven subunits arranged around a sevenfold rotation axis that was itself parallel to the membrane normal. Each monomer consisted of three N-terminal helical regions, denoted TM1 (residues 28 to 60), TM2 (residues 63–90), and TM3, the last of which is composed of TM3a (residues 93 to 113) and TM3b (residues 113 to 128). TM1 and TM2 are connected by a tight turn and TM2 is connected to TM3a by a short loop. The split of TM3 into TM3a and TM3b occurs owing to a kink at G113. TM1, TM2, and TM3a are arranged in a bundle, with TM3b splayed out, akin to a bendy drinking straw. The helical axes of TM1 and TM3a are roughly parallel to each other, with TM2 roughly antiparallel. If one considers the periplasm as being at the top and the cytoplasm as being at the bottom, one moves down the structure from the transmembrane helices to a five-stranded β-sheet domain (residues 133 to 177), followed by a compact domain comprising two α-helices and a three-stranded β-sheet (residues 183 to 199), and finally at the bottom an elongated β-strand (residues 272 to 279). The oligomeric structure is key to understanding the function of the protein (Figure 1d and Figure 2a). The sevenfold rotational arrangement of TM3a forms a tightly packed helical bundle that surrounds the central pore (Figure 2a). The helical axis of each TM3a is offset relative to the membrane normal by about 20°. This central pore is flanked by the seven TM2 helices; the face of each TM2 helix sits against TM1. The seven TM3b helices are arranged tangentially around the central pore, with the helical axis parallel to the membrane. As a result of the sevenfold symmetry, the five-stranded β-sheet domain pairs at each end with a neighboring β-sheet domain; the intersubunit contacts themselves are main chain β-sheet interactions. This results in a continuous circular strip of- β -strands with a diameter >40 Å that wraps around a central cavity; this arrangement of β-strands has been termed a Mobius strip (57). The central cavity is capped at the top by the central pore created by the TM3a helices, and at the bottom the central cavity is enclosed by a ring of the seven compact α/β-domains. Seven 12 Å wide portals into the central cavity are created at the boundaries between the β-sheet domains and the compact α/β-domains. At the very bottom of the cavity, attached to the ring of α/β-domains, is a seven-stranded β-barrel. The side chains attached to the strands fill the internal volume of the β-barrel, suggesting that the barrel does not permit the passage of ions or solutes. A structural role for this feature has been suggested by deletion studies (52; S. Miller & I.R. Booth, unpublished data). The structure of MscS immediately suggests an appealing model in which ions and solutes flow into the central cavity through the portals from the cytoplasm and out through the TM3a pore through the membrane into the periplasm (9).

The crystal structure showed that the narrowest stretch of the pore had a length of about 8 Å and that within this region two rings of Leu side chains (L105 and L109) point inward,

creating two constriction zones in which one lies above the other (9, 37) (Figure 2a). The surface of the pore was uniformly hydrophobic along its length. The initial structure was re-refined with higher-resolution data(3.7 Å)(57).Although this does not significantly change the main chain (cα) trace of the structure, the register (i.e., a specific side chain associated with a specific cα) was corrected for several stretches of residues in the compact domain. In the original paper the channel was considered to be conducting (9) but was reassessed to be closed (57), with the Leu rings creating a pore of less than 5 Å in diameter, as determined by the program HOLE (54) and by Brownian dynamics (68). The closed conformation was in line with a computational analysis (6, 56) that concluded the channel was dewetted and the two rings of Leu act as a vapor lock (6).

This conclusion was shared by a second independent computational analysis (55). Intriguingly, if one examines the structure in detail, the structure is not symmetrical, because the sevenfold rotational symmetry breaks down (Figure 2a). As a result, the closed narrow pore region is not circular, but elliptical. The structure also reports that TM2 helices do not pack tightly against TM3a, and in fact a gap exists (9) (Figure 2a) that could be filled by lipids.

Mutational analysis indicates that the two Leu rings in MscS are critical elements in maintaining the closed state and the gating tension. The mutant, L109S, results in an unstable protein (i.e., accumulating to a lower abundance in the membrane despite transcriptional and translational controls identical to those for the parent protein) that gates at lower tensions (37). Unpublished analysis shows that both L109 and L105 can be substituted with other residues but that normal gating requires the presence of a large hydrophobic residue and that the identity of the L105 residue is critical (S. Black, S. Miller, M.E. Edwards & I.R. Booth, unpublished data). Mutations at L105 have much more deleterious effects than the equivalent mutation at L109 does. These insights correlate well with the variation in pore sequences observed between homologs (Figure 1c).

Was “Closed” Really Shut? New Models Emerge

With the crystal structure apparently representing a closed form of MscS, attention turned to what the open form of the protein might look like and what conformational change occurs between these states. The first proposal based on electrophysiology measurements was termed the dashpot mechanism and surmised that TM3 tilts outward to open the channel (4). This model was expanded by a novel molecular dynamics approach based on extrapolated motion of the closed crystal structure. This approach suggested that the crystal structure was not a true closed state but rather an inactivated nonconducting state (3, 5). The true closed conformation was proposed to have TM3a and TM3b no longer kinked at G113 but instead forming an extended TM3a with a new kink at G121 and consequently a shorter TM3b (Figure 2c). The two rings of Leu still form the plug for the pore, although their relative positions are subtly changed. The assignment of the crystal structure as an inactivated state was based on mutagenesis of both G113 and G121 and a focus on the inactivation and adaption (loss of conductivity) under pressure. The opening of the channel is proposed to result in movement at G121, with the kink disappearing entirely and giving rise to a single TM3 that combines all residues from TM3a and TM3b. This model was extended by the identification of a clutch at L113 and F68 that is proposed to transmit the changein membrane tension to the rest of the protein (10). The finding that the helix-breaking mutation G113P is still capable of function, although it is harder to open and less stable in the open state (19), argues that if such an extended helix forms, it need not be entirely regular.

A combined electron paramagnetic resonance (EPR) molecular dynamics study has also investigated the structure of the closed channel in the lipid environment (66) (Figure 2b).

The EPR approach involves labeling multiple site-directed cysteine mutants with a nitroxide spin label and measuring flexibility, oxygen exposure (as surrogate for lipid embeddedness), Ni2+ ion exposure (as surrogate for water contact), and exposure to a lipid-linked Ni2+ ion (identifies contact with the membrane-water interface) (65, 66). These experimental observations were then used to restrain a standard molecular dynamics simulation starting from the secondary structure observed in the crystal. Conceptually, the approach is similar to protein NMR and was used to determine the open structure of MscL (the first experimental description of an open MS channel) (44, 45). The EPR-restrained structure reveals some differences in the arrangement of the transmembrane helices relative to the crystal structure. TM2 is tilted such that it is more parallel to the membrane normal and is more tightly packed to TM3a [also seen in the novel molecular dynamics models (3)]. TM3b remains profoundly kinked at G113 and adopts a splayed-out conformation similar to that seen in the crystal structure, apparently in disagreement with the extended molecular dynamics model (3). A recent molecular dynamics simulation of the closed form based on EPR coordinates has been reported (35). Although both EPR and dynamics models are different from the original crystal structure, they are guided by a knowledge of the location of residues within the helical regions.

All three structural models favor an explanation of gating that revolves around changes in the transmembrane helices. The protein-centric universe has therefore focused on TM3a and how its structure both permits ion flow (open state) and prevents ion flow (closed state). This has recently been challenged by FRET (Fluoresonance energy transfer) analyses of several mutants in both the β-sheet domain and the α/β-domain (34), which suggest there is significant swelling and conformational change in the cytoplasmic region of the protein during gating. Previous work had identified the significant flexibility of these domains (38), but mutations that remove the lower C-terminal domain, and that should prevent substantial swelling, do not significantly compromise channel gating (52); thus, the significance of these other domains in gating remains unclear.

THE ROLE OF LIPIDS: THE ELEPHANT IN THE ROOM

The Silent Partners that Need More Attention

The lipid bilayer is a complex environment composed, in E. coli, of phosphatidylethanolamine (~74–79%), cardiolipin (~4–8%), and phosphatidylglycerol (~18%) (50). In any lipid bilayer, the head groups are tightly packed together, whereas the fatty acid chains are more fluid. The fluid nature of the membrane is incompatible with the tools that have proven so valuable for our structural understanding of proteins. Consequently, papers that discuss the MS proteins in depth pass over the inconvenient truth that the lipid is the partner to the channel and that one cannot be understood without the other.

Lateral pressure profiles of the bilayer show that the junction between the head group and the lipid chain exhibits the highest tension (22, 46) (Figure 3). The hydrophobic region of the bilayer corresponds to ~32 Å, but it may be less in fully hydrated membranes (31).The glycerol residues and the head groups add a further 30 Å (the data for phosphatidylcholine represent two sets of head groups/bilayer, i.e., 2×15 Å; note that the phosphatidylethanolamine head group is somewhat smaller than phosphatidylcholine owing to the absence of the methyl groups in the latter) (70). The hydrophobic regions of the membrane protein must match the equivalent regions of the bilayer, with the head group region occupied by relatively hydrophilic residues that form hydrogen bonds with the polar components of the glycerol-phosphate-ethanolamine (25, 31). Thus, it is expected in principle that the regions of the channel associated with tensionsensing should lie at this interface region (Figure 3). Sukharev & Corey (59) have speculated that mechanosensitivity

that is solely the property of the channel (i.e., not driven or controlled by ancillary proteins) may have evolved multiple times by “the loosening of constraints” that prevent other proteins from exhibiting mechanosensitive behavior. This theory is supported by properties of specific mutations observed in MscS and MscL (40, 72).

The Lipid-Protein Interface

MscS has three major potential foci for interaction with lipids: the N-terminal sequence (residues 1–27), TM1-2, and TM3b. Depending on which model for MscS is considered, the surface of TM3a that faces the bilayer may interact with lipids of the inner leaflet, but this remains untested. Genetic evidence suggests that the residues close to the N terminus (residues 1–27) do influence channel gating (48, 65, 66). The clearest evidence comes from analysis of the Trp residue at position 16 in E. coli MscS. Substitutions with similar residues (Phe, Tyr, Leu) cause a progressive reduction in pressure sensitivity (i.e., the mutant channels require higher pressures for the closed-to-open transition) (48). The failure to locate these residues in the crystal structure is an important deficiency of the structure.

TM3b is amphipathic, and in the crystal structures the hydrophobic residues project toward the bilayer, potentially allowing this helix to reside in the head group region to ensure that the hydrophobic residues contact the lipid chains. The head group region is deep enough to accommodate an α-helix (70), making this arrangement feasible. At the end of TM3b are relatively conserved Arg residues (Arg128 and Arg131), either of which can bond to the phosphate head groups of the bilayer, thus providing a peripheral anchor for the vestibule of MscS. An analysis of mutants within TM3b has been somewhat limited and has concentrated on the possibility of Arg128 and Arg131 forming salt bridges to TM1-TM2 through Asp62 (41, 55).

The TM1-TM2 interface region is situated within the lipid bilayer and therefore is likely the major focus for tension sensing (though important contributions from TM3b and the N terminus are not ruled out). In both MscS and MscL, mutations that inhibit gating are frequently located close to the boundary between the head groups and the lipid chains, suggesting that this is a critical region for sensing tension (40, 42, 72) (Figure 3). We have previously suggested (15) that mechanosensing behavior is due to the absence rather than the presence of specific residues (35). Amino acid substitutions that inhibit MscS and MscL gating replace hydrophobic residues at the interface with those that favor hydrogen bonding (40). Conversely, similar substitutions into the transmembrane helices of MscS, at positions predicted to lie deeper into the lipid phase, cause channels to gate at lower membrane tensions (40, 42). These mutations affect changes in TM1 and TM2. Tension sensing may thus be seen as a reduced frequency of residues, at the TM1-TM2 interface region, that favor hydrogen bonding. In contrast, the presence of these mutations elsewhere in the transmembrane helices may help set the tension at which the channel gates. In nonmechanosensitive membrane proteins there is an enrichment of residues that favor hydrogen-bond formation with the lipid head groups at the interface region. Such residues have been suggested, on the basis of structural studies, to stabilize the proteins in the bilayer (25, 31, 67). Thus, such proteins fail to exhibit significant structural transitions in response to changes in membrane tension, whereas MscS and MscL undergo rearrangements to create open pores.

BREACHING THE BARRIER: OPENING THE CHANNEL

Experiments to Address Channel Opening

Two major techniques, patch clamp electrophysiology (36) and survival experiments (32, 37, 38), allow the investigation of MS channel activity and are frequently used to evaluate mutants. Patch clamping enables investigators to study single channel properties and to

define core properties, including pressure sensitivity, conductance, open dwell time, and inactivation rate. These properties are determined most frequently on membrane patches derived from cells grown at low osmolarity (36). However, the core properties of MscS have also been verified by purification and reconstitution (58). Survival experiments provide a less robust, indicative analysis of MS channel activity. Cells grown at high osmolarity are diluted rapidly into media of lower osmolarity, and the population is plated onto media and incubated to allow colonies to form. The survival rate of the shocked population is an indication of channel function. A more detailed consideration of this assay has been published elsewhere (14). It should be noted, however, that the two channel assays utilize membranes from different growth regimes that themselves affect lipid composition (50). Two additional critical factors are that there is not a linear relationship between channel abundance and survival and that mutant channels with widely divergent properties can provide similar protection against downshock. Failure to protect in a downshock assay can result either from total loss of function or from gain of function; in the latter the frequent gating of the channel inhibits growth (14, 37).

Mutagenesis is a deceptively simple approach to protein structure-function relationships. However, all mutations modify the character of the protein into which they are introduced. The great advantage of this approach, beyond its simplicity, is the option to substitute any residue with the other 19. Rarely is the technique taken to this extreme. Critically, the mutant protein is clearly not the wild type—it now possesses introduced properties, some of which are discernible through analysis, others are more subtle (see, for example, Reference 48). In some cases the mutational change is the first step in an experimental stratagem, such as the introduction of Cys residues into anchor spin probes (44, 65, 66) or Trp insertion to create a fluorescence reporter (48, 49).

The analysis of mutants has been used to great effect to identify critical elements of gating, but care must be taken to remember that such analysis reports on the mutant protein, not the parent. A rigorous analysis must consider both what residue has been removed and what has been inserted in its place. Some amino acids are good substitutes, hence the popularity of alanine-scanning. The small size and hydrophobicity of this amino acid make relatively simple inferences possible. In contrast, polar amino acids, such as serine, generate novel hydrogen bonds both within helices (kinking) and between helices (1, 2). For MscS the comparison of Ala and Ser mutations at the same positions in TM3a illustrates this (20). Introduction of Ala into TM3a makes the channel harder to gate, but a Ser residue at the same position makes the channel gate more easily; the potential for misinterpretation is therefore high. Residue bulk is not substantially different, but the propensity for adventitious hydrogen bond formation is much greater for Ser. Consequently, the effects of introducing Ser residues may have more to do with their helix-breaking tendencies than with their bulk. Interpreting Ser mutants in the absence of other data is particularly challenging.

Raising the Floodgate: Models for Gating

A range of techniques has led to considerable focus on the closed-to-open transition (5, 10, 20, 34, 40, 42, 65, 66, 69). However, the most systematic approach has been the application of site-directed mutagenesis to the TM3a and TM3b helices. Bass et al. (9) noted that the E. coli MscS TM3a helices exhibited a conserved pattern of Gly and Ala residues (98-AXXGAAGXAXGXAXZG- 113; E. coli MscS numbering; where X is a hydrophobic residue and Z is hydrophilic) that in the crystal structure were opposed to each other in a knobs and grooves pattern (Figure 1d). It was subsequently proposed that the symmetrical heptamer exhibited helices that were packed as tightly as possible (though tighter packing can be achieved by collapsing the symmetry to create an asymmetric seven-helix bundle) (26, 27, 54). This generated a model in which the helices might slide across each other to attain the open state (20). Introduction of bulky side chains was predicted to inhibit this

structural transition, and side chain removal (Ala to Gly mutations) was predicted to facilitate the helix sliding. Indeed, side chain removal by substituting Ala with Gly led to channels that gated more easily (20). Conversely, replacement of the Gly residues at positions 101, 104, and 108 with Ala residues resulted in channels that were intrinsically more resistant to pressure, and gating events were rare, even when the protein was abundant in the membrane (20).

Similar observations were made with Ala to Val or Ala to Leu mutations in which the bulk of the side chain is also increased. Moreover, in many such mutants the open state of the channel exhibited a lowered conductance. This property is particularly marked in an A106V mutant that was subsequently crystallized in an open state (69). Thus, A106V is a fully functional channel as determined by survival experiments, but in patch clamp it exhibits unusual properties that suggested it as a candidate for crystallography. At low pressures A106V required slightly more pressure to open and exhibited short-duration openings (~4 ms versus 150 ms), but the conductance was equivalent to that of the parent channel (20, 69). These properties are consistent with the model in which the greater bulk inhibits the transition to the open state and makes the open state significantly less stable. However, at higher pressures A106V channels exhibited stable openings but with a 30% reduction in conductance (20). A reduction of this magnitude suggests that the subconducting state would have an estimated pore diameter of 10 to 13 Å, intermediate between that calculated for the closed (5 Å) and open (14 to 16 Å) forms.

Mutant cycle analysis, in which single and double mutants were created and analyzed, showed two core properties of the MscS pore helices. First, as long as the surfaces are complementary it does not matter which helix bears the knob and which the groove (20, 69). Thus, a G108A mutation caused the MscS protein to be relatively poorly expressed and difficult to open. In contrast, an A106G mutation expressed normally, opened easily, but exhibited a reduced conductance. Combining the two mutations led to a channel that was accumulated to normal abundance, gated in the normal range of pressures, and exhibited conductance close to that of the wild type. The positions of the Ala and Gly residues of this double mutant are exchanged on the helix interface, thus confirming the importance of surface complementarity (20). Second, TM3a helices exhibit summation properties. Although TM3a helices pack Ala against Gly of the adjacent helix, substitutions at one register in the helix may compensate for changes at another register even when there is no capacity for the two amino acid side chains to interact directly (Figure 1d). For example, an A106G mutation gates readily at low pressure and it can be compensated by G101A, G104A, or G108A. Based on the crystal structure, only G108A can have an immediate direct interaction, indicating that the effects of G101A and G104A most likely accrue from summation of the energy barriers required to be overcome for gating. Similarly, critical position-specific suppression effects can be seen when studying double mutants created from an L109A seal mutant (S. Black, M.D. Edwards, S. Miller & I.R. Booth, unpublished data). These observations may bear upon the divergences from the conserved TM3a motif, observed in other MscS homologs that exhibit modified gating pressures and conductance (M.D. Edwards, S. Black, S. Miller, & I.R. Booth, unpublished data). Multiple solutions provide a working interface between helices that allows gating, even to the extent of the presence of the bulky Trp side chain in TM3a of some homologs (Figure 1c).

The Adaptation Phenomenon: Coping with Constant Pressure

Structurally, the process of adaptation, i.e., loss of conductivity under pressure, is hard to understand (4, 5, 11, 13, 15, 32). By its nature adaptation seems to be a stochastic process: Channels, which flicker between open and closed states, decay to a nonconducting state with a certain half-life. It is not clear whether all the different inactive forms observed with parent and mutant channels are in the same physical state, because the resolution of the data is

poor. Moreover, there is no strong evidence that adaptation is evolutionarily conserved across the MscS family, whether one considers just the members of that family closely related to E. coli MscS or the much wider family (32, 33). The physiological significance of inactivation is also debatable (15) because the time frames of the process are much longer than the physiological response. Probing the phenomenon has relied on mutant channels to prove significance, which is an unreliable strategy (see above). Static models are poor guides to events with low frequency, and no reliable structural model of inactivation exists. Creating an open pore must involve the outward movement of the TM3a helices to create the wider pore (20, 58, 69). The A106V structure (Figure 4a) suggested a route by which this might be achieved (69). The TM3a helices are not tightly packed in this structure, and alternating between the tightly packed (closed) and non-tightly packed (open) helices could, like protein folding, result in trapped conformations (69). Experimental support (e.g., mutations that increased cycling rate) for this model was produced but is far from conclusive (19, 69). Understanding the meaning and significance of the inactivated state(s) awaits new techniques that can provide greater insight.

STRUCTURAL BIOLOGY DIVERGES

How to Study the Structure of an Open Channel

Obtaining structural insights into the open form of MscS is challenging. No system exists that combines the membrane tension needed to open the channel with tractability to the most powerful experimental tools for structure determination (crystallography, NMR, electron microscopy). The closest experimental system is that pioneered for the EPR/molecular dynamics study of MscL (44, 45). This method embeds the protein in a liposome to mimic the natural lipid bilayer. The open conformation of the channel was obtained by adding the lipid 1-tetradecanoyl-glycero-3-phosphocholine (lysoPC) to the liposomes; its asymmetric incorporation into the vesicles results in channel openings similar to those seen under pressure (45). This approach revealed the structure of an open form of MscS (65) (Figure 4b), and similar to the molecular dynamics model (3), it shows that TM3a expands outward in a motion that is coupled to TM1 and TM2 (Figure 4c).

However, in contrast to the molecular dynamics model (3), the EPR model shows TM3a and TM3b remain kinked at G113, although there is some motion within TM3b (Figure 4b,c). The EPR model shows that TM3a undergoes a one-quarter rotation and translation about its own axis. As a result the helices superimpose with the other models, but the superimposed residues are shifted by one (i.e., Leu105 in the open EPR structure superimposes with G104 in the other structures). This radical rotation of TM3a opens the channel.

Competing Models for Channel Opening

When the open EPR model was reported, a second crystal structure of MscS (an A106V mutant) at 3.45 Å resolution was reported (69) (Figure 4a). This structure showed an arrangement of the transmembrane helices different from that seen in the original MscS structure. TM1 and TM2 were rotated by almost one-seventh of a revolution, and the helical axis of TM3a tilted by approximately 20° to become parallel to the membrane normal and slightly rotated. TM3b and the cytoplasmic domain did not appear to have changed greatly from the original structure. As a result of the motions of TM3a the two Leu rings are rotated and moved out of the pore, creating a pore diameter of 13 Å,close to earlier predictions that an increase in pore size of 8 Å was needed to obtain full conductivity (6, 58). This diameter is within the range calculated for the diameter of the subconducting state of A106V MscS. The extrapolated molecular dynamics model gives a wider pore diameter of 15.2 Å using the same parameters as those used for the crystal structure (Figure 4c). The TM3a structures are also no longer tightly packed, as was seen in the closed crystal structure. As noted above,

this may relate to the adaptation phenomenon (69). Whether these gaps between TM3a in the crystal structure are filled partly by lipids remains unanswered. Like the native structure, TM2 does not tightly pack against TM3a (Figure 2a). The A106V MscS mutant structure was considered to be an open form of the channel (69). The mutation was proposed to destabilize the closed form of the protein seen in original crystal structure by introducing a clash at TM3a and thus preventing this form from crystallizing. Because 106V does not contact any residue in the open structure, it was suggested that it did not specifically stabilize the open form observed in the crystal. The paper proposed a model for channel gating in which TM1 and TM2 sense the change in membrane tension and move (rotate and tilt) in response. These changes act upon TM3a, which pivots at G113 against TM3b (which remains anchored to the membrane) (69). The paper points out that the pivot motion does not require any special backbone conformations at G113 and thus is consistent with activity of G113 mutants (69).

Structural analysis has identified two locations, one between L115 and A110 (termed the switch) and a second between A102 and G104, that would undergo significant change during the proposed gating movement of TM3b (69). The gating model requires the side chain of A110 to slip over the side chain of L115. Thus, mutations that increase the size of either side chain were predicted to make it harder to open the channel, whereas those that made either side chain smaller were predicted to make it easier to open but would also likely make the open channel less stable (69). The authors reported multiple mutations at A110 and L115, all of which were consistent with this proposition (69). The gating model predicts that the methyl group of the side chain of A102 moves across the surface of a neighboring helix, particularly the residue G104 (20, 69). By transferring the methyl group from one to chain to another, a double mutant, A102G G104A, should therefore be essentially wild type, whereas each single mutant would show perturbed behavior. This mutant cycle analysis has proven particularly powerful in interpreting MscS behavior (20, 69; S. Black, S. Miller & M.D. Edwards, unpublished data). The various mutations were made and tested and the predictions held true (69). A comparison of A106V MscS with the EPR-derived open structure (65) (Figure 4b) reveals similar movement of TM3a outward from the pore but different movements of TM1-TM2 upon opening, leading to a different model for gating. The EPR model locates the N-terminal 25 residues (once again not resolved in the crystal structure), which play an important role in channel function (48, 65, 66).

The Problems with Current Approaches

The A106V structure (like the original crystal structure) has been criticized as being unrepresentative of the physiological state (5, 11, 13). The criticism focuses on the following points: (a) The N-terminal 25 residues are not identified in the crystals, and as we have discussed above, these play an important role (48, 65, 66). (b) The measured conductivity of open MscS is higher than that predicted from a simulation of conductivity of the A106V structure (29) (i.e., A106V is not open enough). (c) The non-tight-packing arrangement of the TM2 and TM3a seen in both crystals structures is claimed to be precluded by molecular modeling (10), and the kinking at G113 seen in both structures is held to be incompatible with the inactivation rate of the G113A mutant (3). Some of these issues remain open questions, because no definitive experiments have addressed the issue; others have been investigated and their outcome is described above. The EPR models (65, 66) have not attracted the same detailed critique, and they differ significantly from the extrapolated dynamics models (5) (Figure 4c).

CONCLUSIONS

Future Prospects: An Open Book?

Three competing structural models for gating bedevil our structural understanding of MscS. All the models are advanced with varying degrees of support from site-directed mutagenesis. This is a serious problem, because formulation of hypotheses and rationalization of biological data have three different models from which to choose. It appears certain that further calculation and site-directed mutagenesis will not definitively resolve which, if any, model is closest to the real situation. Some new technique orthogonal to the existing approaches is urgently required. Resolving this conundrum is critical for our understanding of not only MscS, since all three techniques are being applied to other membrane proteins. Such unresolved contradictions are antithetical to progress. MscS remains, to date, the only ion channel to be studied by all three techniques in both the open and closed forms. Of the three techniques, the flaws in crystallography are easiest to identify. The protein undergoes two large changes: removal from the lipid bilayer and packing inside a crystal. Each or both of these events could plausibly allow or indeed force the protein to adopt a nonnatural conformation. If this is true for MscS, it could well be true for many other membrane proteins, thus questioning the value of the resource expended for the crystallization of such proteins. The EPR approach works with a physiologically relevant state but requires extensive mutation and restraint against qualitative data. The approach is, however, widely applicable. It deserves more widespread use if it can be shown to be more informative than crystallography. Further, it would be an invaluable adjunct to crystallography, permitting the correction of any artifacts introduced into structures by crystallization. If the crystal structure is closer to reality, the EPR approach, although giving valuable low-resolution information, may give errors in detail and thus require further experimental data to validate its models. Authors studying EPR have cautioned that the technique does not reliably position side chains and have carefully avoided overinterpreting their structural data (45, 65, 66). The dangers inherent to limited datasets derived from site-directed mutagenesis have already been alluded to, but mutagenesis remains the keystone of hypothesis testing. Molecular dynamics has provided many important contributions to how we think about MS channels in general and MscS in particular. The most beneficial outcome for science would be if new molecular dynamics approaches resulted in models that were closer to reality than the models of either experimental approach are. It would greatly reduce the need for technically demanding EPR and crystallization (which suffers from the additional drawback of being inconsistent). Further, computational models would allow investigators to assess the lipid environment, a crucial component of channel function (31). Here crystallography is rarely helpful because the lipid is largely removed from the membrane protein to aid crystallization. Thus, structural biology has generally been distinguished only by its silence. However, if the in silico approach is at odds with reality, this would caution against the widespread use of such simulations until there is some further refinement of force fields.

Acknowledgments

We are very grateful to Professors Perozo and Sukharev for providing the coordinates for their models for closed and open states of MscS. The authors thank members of their research groups who have contributed substantially to the progress of this research area and who have provided assistance with figures. Their individual contributions are acknowledged through appropriate citations and references to unpublished work. The Wellcome Trust (WT092552MA) has made our research possible for almost 20 years, and we are grateful for their support.

Abbreviations

Mechanosensitive (MS)	responding to the change in the lateral tension of the lipid bilayer.

MscS	mechanosensitive channel of small conductance
MscM	mechanosensitive channel of mini conductance
Gating	the transition from the open form to the closed form of the channel
MscL	mechanosensitive channel of large conductance
Amphipathic helix	a helix that displays hydrophobic residues on one side and hydrophilic residues on the other
Transmembrane(TM) helix	a piece of secondary structure that penetrates the lipid bilayer
Ion channel	a route made by a protein for ions or solvated ions to pass through the otherwise impermeable membrane
EPR	electron paramagnetic resonance

References

1. Adamian L, Jackups R Jr, Binkowski TA, Liang J. Higher-order interhelical spatial interactions in membrane proteins. J. Mol. Biol. 2003; 327:251–72. [PubMed: 12614623]
2. Adamian L, Liang J. Interhelical hydrogen bonds and spatial motifs in membrane proteins: polar clamps and serine zippers. Proteins. 2002; 47:209–18. [PubMed: 11933067]
3. Akitake B, Anishkin A, Liu N, Sukharev S. Straightening and sequential buckling of the pore-lining helices define the gating cycle of MscS. Nat. Struct. Mol. Biol. 2007; 14:1141–49. [PubMed: 18037888] - Reports extended dynamics analysis of MscS in both open and closed forms and focuses on the kinking and unkinking within TM3b.
4. Akitake B, Anishkin A, Sukharev S. The“dashpot”mechanismofstretch-dependentgatinginMscS. J. Gen. Physiol. 2005; 125:143–54. [PubMed: 15657299]
5. Anishkin A, Akitake B, Sukharev S. Characterization of the resting MscS: modeling and analysis of the closed bacterial mechanosensitive channel of small conductance. Biophys. J. 2008; 94:1252–66. [PubMed: 17981908]
6. Anishkin A, Sukharev S. Water dynamics and dewetting transitions in the small mechanosensitive channel MscS. Biophys. J. 2004; 86:2883–95. [PubMed: 15111405]
7. Anishkin A, Sukharev S. State-stabilizing interactions in bacterial mechanosensitive channel gating and adaptation. J. Biol. Chem. 2009; 284:19153–5. [PubMed: 19383606]
8. Bartlett JL, Levin G, Blount P. An in vivo assay identifies changes in residue accessibility on mechanosensitive channel gating. Proc. Natl. Acad. Sci. USA. 2004; 101:10161–65. [PubMed: 15226501]
9. Bass RB, Strop P, Barclay M, Rees DC. Crystal structure of *Escherichia coli* MscS, a voltage-modulated and mechanosensitive channel. Science. 2002; 298:1582–87. [PubMed: 12446901] - Produces the key insight into the channel organization, showing it was heptameric and identifying the transmembrane helices.
10. Belyy V, Anishkin A, Kamaraju K, Liu N, Sukharev S. The tension-transmitting ‘clutch’ in the mechanosensitive channel MscS. Nat. Struct. Mol. Biol. 2010; 17:451–58. [PubMed: 20208543]
11. Belyy V, Kamaraju K, Akitake B, Anishkin A, Sukharev S. Adaptive behavior of bacterial mechanosensitive channels is coupled to membrane mechanics. J. Gen. Physiol. 2010; 135:641–52. [PubMed: 20513760]
12. Berrier C, Coulombe A, Houssin C, Ghazi A. A patch-clamp study of ion channels of inner and outer membranes and of contact zones of *E. coli*, fused into giant liposomes. Pressure-activated channels are localized in the inner membrane. FEBS Lett. 1989; 259:27–32. [PubMed: 2480919]
13. Boer M, Anishkin A, Sukharev S. Adaptive MscS gating in the osmotic permeability response in *E. coli*: the question of time. Biochemistry. 2011; 50:4087–96. [PubMed: 21456519]

14. Booth IR, Edwards MD, Black S, Schumann U, Bartlett W, et al. Physiologicalanalysi sofbacterial mechanosensitive channels. Methods Enzymol. 2007; 428:47–61. [PubMed: 17875411]
15. Booth IR, Edwards MD, Black S, Schumann U, Miller S. Mechanosensitive channels in bacteria: signs of closure? Nat. Microbiol. 2007; 5:431–40.
16. Booth IR, Louis P. Managing hypoosmotic stress: aquaporins and mechanosensitive channels in *Escherichia coli*. Curr. Opin. Microbiol. 1999; 2:166–69. [PubMed: 10322175]
17. Britten RJ, McClure FT. The amino acid pool of Escherichia coli. Microbiol.Mol.Biol. Rev. 1962; 26:292–335.
18. Cruickshank CC, Minchin RF, Le Dain AC, Martinac B. Estimation of the pore size of the large-conductance mechanosensitive ion channel of *Escherichia coli*. Biophys. J. 1997; 73:1925–31. [PubMed: 9336188]
19. Edwards MD, Bartlett W, Booth IR. Pore mutations of the *Escherichia coli* MscS channel affect desensitization but not ionic preference. Biophys. J. 2008; 94:3003–13. [PubMed: 18065458]
20. Edwards MD, Li Y, Kim S, Miller S, Bartlett W, et al. Pivotal role of the glycine-rich TM3 helix in gating the MscS mechanosensitive channel. Nat. Struct. Mol. Biol. 2005; 12:113–19. [PubMed: 15665866] - Identifies interactions between residues on the pore helix, leading to a proposal of helices sliding across each other during channel gating.
21. Felle H, Porter JS, Slayman CL, Kaback HR. Quantitative measurements of membrane potential in *Escherichia coli*. Biochemistry. 1980; 19:3585–90. [PubMed: 6996707]
22. Gullingsrud J, Schulten K. Lipid bilayer pressure profiles and mechanosensitive channel gating. Biophys. J. 2004; 86:3496–509. [PubMed: 15189849]
23. Hamill OP, McBride DW. The cloning of a mechano gated membrane ion channel. Trends Neurosci. 1994; 17:439–43. [PubMed: 7531881]
24. Haswell ES, Meyerowitz EM. MscS-like proteins control plastid size and shape in *Arabidopsis thaliana*. Curr. Biol. 2006; 16:1–11. [PubMed: 16401419]
25. Killian JA, von Heijne G. How proteins adapt to a membrane-water interface. Trends Biochem. Sci. 2000
26. Kim S, Chamberlain AK, Bowie JU. Asimplemethodformodelingtransmembranehe lixoligomers. J. Mol. Biol. 2003; 329:831–40. [PubMed: 12787681]
27. Kim S, Chamberlain AK, Bowie JU. Membrane channel structure of *Helicobacter pylori* vacuolating toxin: role of multiple GXXXG motifs in cylindrical channels. Proc. Natl. Acad. Sci. USA. 2004; 101:5988–91. [PubMed: 15067113]
28. Kung C. A possible unifying principle for mechanosensation. Nature. 2005; 436:647–54. [PubMed: 16079835]
29. Kung C, Martinac B, Sukharev S. Mechanosensitive channels in microbes. Annu. Rev. Microbiol. 2010; 64:313–29. [PubMed: 20825352]
30. Kyte J, Doolittle RF. A simple method for displaying the hydropathic character of a protein. J.Mol. Biol. 1982; 157:105–32. [PubMed: 7108955]
31. Lee AG. Lipid-protein interactions in biological membranes: a structural perspective. Biochim. Biophys. Acta. 2003; 1612:1–4032. [PubMed: 12729927]
32. Levina N, Totemeyer S, Stokes NR, Louis P, Jones MA, Booth IR. Protection of *Escherichia coli* cells against extreme turgor by activation of MscS and MscL mechanosensitive channels: identification of genes required for MscS activity. EMBO J. 1999; 18:1730–37. [PubMed: 10202137] – Identifies MscS and establishes the significance of MS channels, marking the field as critical in understanding bacterial physiology.
33. Li Y, Moe PC, Chandrasekaran S, Booth IR, Blount P. Ionic regulation of MscK, a mechanosensitive channel from *Escherichia coli*. EMBO J. 2002; 21:5323–30. [PubMed: 12374733]
34. Machiyama H, Tatsumi H, Sokabe M. Structural changes in the cytoplasmic domain of the mechanosensitive channel MscS during opening. Biophys. J. 2009; 97:1048–57. [PubMed: 19686652]
35. Malcolm HR, Heo YY, Elmore DE, Maurer JA. Defining the role of the tension sensor in the mechanosensitive channel of small conductance. Biophys. J. 2011; 101:345–52. [PubMed: 21767486]

36. Martinac B, Buehner M, Delcour AH, Adler J, Kung C. Pressure-sensitive ion channel in *Escherichia coli*. Proc. Natl. Acad. Sci. USA. 1987; 84:2297–301. [PubMed: 2436228] Provides the first definitive identification of the MscS ion channel and is the bedrock of the field.
37. Miller S, Bartlett W, Chandrasekaran S, Simpson S, Edwards M, Booth IR. Domain organization of the MscS mechanosensitive channel of *Escherichia coli*. EMBO J. 2003; 22:36–46. [PubMed: 12505982] - Identifies first gain-of-function mutants (that open more easily) and establishes the importance of leucine rings in gating and structure.
38. Miller S, Edwards MD, Ozdemir C, Booth IR. The closed structure of the MscS mechanosensitive channel cross-linking of single cysteine mutants. J. Biol. Chem. 2003; 278:32246–50. [PubMed: 12767977]
39. Nakayama Y, Fujiu K, Sokabe M, Yoshimura K. Molecular and electrophysiological characterization of a mechanosensitive channel expressed in the chloroplasts of *Chlamydomonas*. Proc. Natl. Acad. Sci. USA. 2007; 104:5883–884. [PubMed: 17389370]
40. Nomura T, Sokabe M, Yoshimura K. Lipid-protein interaction of the MscS mechanosensitive channel examined by scanning mutagenesis. Biophys. J. 2006; 91:2874–81. [PubMed: 16861270] Demonstrates that insertion of hydrogen-bonding amino acids into TM1-2 of MscS caused inhibition of gating
41. Nomura T, Sokabe M, Yoshimura K. Interaction between the cytoplasmic and transmembrane domains of the mechanosensitive channel MscS. Biophys. J. 2008; 94:1638–45. [PubMed: 17993482]
42. Okada K, Moe PC, Blount P. Functional design of bacterial mechanosensitive channels. Comparisons and contrasts illuminated by random mutagenesis. J. Biol. Chem. 2002; 277:27682–88. [PubMed: 12015316]
43. Perozo E. Gating prokaryotic mechanosensitive channels. Nat. Rev. Mol. Cell Biol. 2006; 7:109–19. [PubMed: 16493417]
44. Perozo E, Cortes DM, Sompornpisut P, Kloda A, Martinac B. Open channel structure of MscL and the gating mechanism of mechanosensitive channels. Nature. 2002; 418:942–48. [PubMed: 12198539] - describes an open structure for MscL based on EPR analysis of the channel embedded in the lipid bilayer.
45. Perozo E, Kloda A, Cortes DM, Martinac B. Physical principles underlying the transduction of bilayer deformation forces during mechanosensitive channel gating. Nat. Struct. Biol. 2002; 9:696–703. [PubMed: 12172537]
46. Perozo E, Rees DC. Structure and mechanism in prokaryotic mechanosensitive channels. Curr. Opin. Struct. Biol. 2003; 13:432–42. [PubMed: 12948773]
47. Pivetti CD, Yen MR, Miller S, Busch W, Tseng YH, et al. Two families of mechanosensitive channel proteins. Microbiol. Mol. Biol. Rev. 2003; 67:66–85. [PubMed: 12626684]
48. Rasmussen A, Rasmussen T, Edwards MD, Schauer D, Schumann U, et al. The role of tryptophan residues in the function and stability of the mechanosensitive channel MscS from *Escherichia coli*. Biochemistry. 2007; 46:10899–908. [PubMed: 17718516]
49. Rasmussen T, Edwards MD, Black SS, Rasmussen A, Miller S, Booth IR. Tryptophan in the pore of the mechanosensitive channel MscS: assessment of pore conformations by fluorescence spectroscopy. J. Biol. Chem. 2010; 285:5377–84. [PubMed: 20037156]
50. Romantsov T, Guan Z, Wood JM. Cardiolipinandtheosmoticstressresponsesofbacteria. Biochim. Biophys. Acta. 2009; 1788:2092–100. [PubMed: 19539601]
51. Ruthe HJ, Adler J. Fusionofbacterialspheroplastsbyelectricfields. Biochim.Biophys.Acta. 1985; 819:105–13. [PubMed: 3899175]
52. Schumann U, Edwards MD, Li C, Booth IR. The conserved carboxy-terminus of the MscS mechanosensitive channel is not essential but increases stability and activity. FEBS Lett. 2004; 572:233–37. [PubMed: 15304354]
53. Schumann U, Edwards MD, Rasmussen T, Bartlett W, van West P, Booth IR. YbdG in *Escherichia coli* is a threshold-setting mechanosensitive channel with MscM activity. Proc. Natl. Acad. Sci. ŮSA. 2010; 107:12664–69.

54. Smart OS, Neduvelil JG, Wang X, Wallace BA, Sansom MS. HOLE: a program for the analysis of the pore dimensions of ion channel structural models. J. Mol. Graph. 1996; 14:354–60. 76. [PubMed: 9195488]
55. Sotomayor M, Schulten K. Molecular dynamics study of gating in the mechanosensitive channel of small conductance MscS. Biophys. J. 2004; 87:3050–65. [PubMed: 15339798]
56. Sotomayor M, Vasquez V, Perozo E, Schulten K. Ion conduction through MscS as determined by electrophysiology and simulation. Biophys. J. 2007; 92:886–902. [PubMed: 17114233]
57. Steinbacher S, Bass R, Strop P, Rees DC. Structures of the prokaryotic mechanosensitive channels MscL and MscS. Curr. Top. Membr. 2007; 58:1–24.
58. Sukharev S. Purification of the small mechanosensitive channel of *Escherichia coli* (MscS): the subunit structure, conduction, and gating characteristics in liposomes. Biophys. J. 2002; 83:290–98. [PubMed: 12080120] - Demonstrates that MscS can be purified and assayed on its own
59. Sukharev S, Corey DP. Mechanosensitive channels: multiplicity of families and gating paradigms. Sci. STKE. 2004; 2004:re4. [PubMed: 14872099]
60. Sukharev SI, Blount P, Martinac B, Blattner FR, Kung C. A large-conductance mechanosensitive channel in *E. coli* encoded by *mscL* alone. Nature. 1994; 368:265–68. [PubMed: 7511799]
61. Sukharev SI, Martinac B, Arshavsky VY, Kung C. Two types of mechanosensitive channels in the *Escherichia coli* cell envelope: solubilization and functional reconstitution. Biophys. J. 1993; 65:177–83. [PubMed: 7690260]
62. Szabo I, Petronilli V, Zoratti M. A patch-clamp study of *Bacillus subtilis*. Biochim. Biophys. Acta. 1992; 1112:29–38. [PubMed: 1384708]
63. Szabo I, Petronilli V, Zoratti M. A patch-clamp investigation of the *Streptococcus faecalis* cell membrane. J. Membr. Biol. 1993; 131:203–18. [PubMed: 7684083]
64. Touze T, Gouesbet G, Bolangiu C, Jebbar M, Bonnassie S, Blanco C. Glycine betaine loses its osmoprotective activity in a bspA strain of *Erwinia chrysanthemi*. Mol. Microbiol. 2001; 42:87–99. [PubMed: 11679069]
65. Vasquez V, Sotomayor M, Cordero-Morales J, Schulten K, Perozo E. A structural mechanism for MscS gating in lipid bilayers. Science. 2008; 321:1210–14. [PubMed: 18755978]
66. Vasquez V, Sotomayor M, Cortes DM, Roux B, Schulten K, Perozo E. Three-dimensional architecture of membrane-embedded MscS in the closed conformation. J. Mol. Biol. 2008; 378:55–70. [PubMed: 18343404]
67. Vonheijne G. Principles of membrane protein assembly and structure. Prog. Biophys. Mol. Biol. 1996; 66:113–39. [PubMed: 9175426]
68. Vora T, Corry B, Chung SH. Brownian dynamics investigation into the conductance state of the MscS channel crystal structure. Biochim. Biophys. Acta. 2006; 1758:730–37. [PubMed: 16781663]
69. Wang W, Black SS, Edwards MD, Miller S, Morrison EL, et al. The structure of an open form of an *E. coli* mechanosensitive channel at 3.45 Å resolution. Science. 2008; 321:1179–83. [PubMed: 18755969] - Describes an open structure of MscS and proposes and tests a detailed model for the structural changes during gating.
70. White SH, Ladokhin AS, Jayasinghe S, Hristova K. How membranes shape protein structure. J. Biol. Chem. 2001; 276:32395–98. [PubMed: 11432876]
71. Wilson ME, Jensen GS, Haswell ES. Two mechanosensitive channel homologs influence division ring placement in *Arabidopsis* chloroplasts. Plant Cell. 2011; 23:2939–49. [PubMed: 21810996]
72. Yoshimura K, Nomura T, Sokabe M. Loss-of-function mutations at the rim of the funnel of mechanosensitive channel MscL. Biophys. J. 2004; 86:2113–20. [PubMed: 15041651]
73. Zoratti M, Petronilli V, Szabo I. Stretch-activated composite ion channels in Bacillus subtilis.Biochem. Biophys. Res. Commun. 1990; 168:443–50.

Europe PMC Funders Author Manuscripts

SUMMARY

1. MscS is a transmembrane protein that functions as a nonspecific mechanosensitive channel.
2. MscS opens in response to pressure inside the bacterial cell (turgor pressure), relieving the pressure before the cell ruptures.
3. MscS is a hepatamer with three transmembrane helices and a large cytoplasmic soluble domain.
4. The major member of the MscS family that has been studied is one of the smaller homologs (286 amino acids); members of the family can be as large as 1,120 amino acids.
5. There is considerable debate about the closed form of the structure in cells, with crystallography data differing from both modeling and EPR (which also differ from each other) data.
6. Site-directed mutagenesisis a valuable mechanism of hypothesis testing and has identified key residues required for channel gating.
7. Structural descriptions of the open channel have been produced by three techniques that unfortunately lead to different models of gating.
8. Resolving which, if any, of these models most closely resembles reality is a key challenge for biophysics.

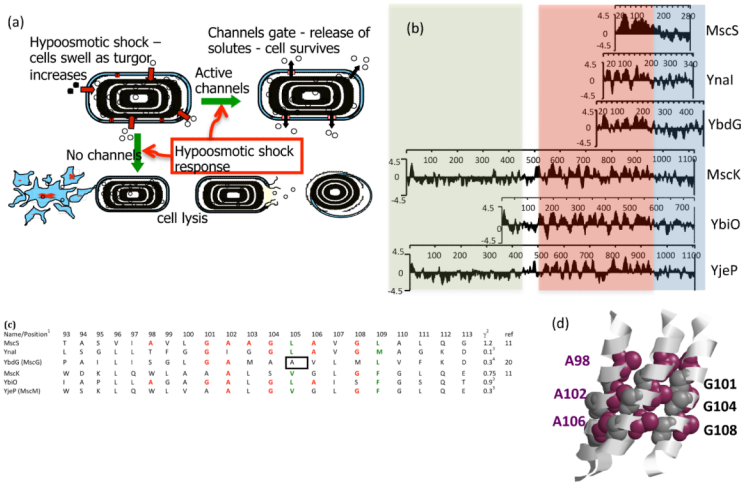

Fig 1.

Variation and function in mechanosensitive channel of small conductance (MscS) channel homologs. (a) Mechanosensitive (MS) channels protect against cell lysis during hypoosmotic shock (downshock). During growth at high osmolarity, bacterial cells accumulate high levels of solute. Transfer to a dilute medium results in rapid inrush of water that requires the activation of the channels to elicit solute egress from the cell. Failure of channels to be activated leads to cell lysis, resulting in a number of distinct forms (left to right): fragments, viable cells, cell-like ghosts, and empty sacs (figure adapted from M. Reuter, N. Hayward, S. Miller, D. Dryden & I.R. Booth, unpublished data). (b) Homologs of MscS exhibit varying sizes, owing principally to extensions at the N terminus. The figure shows the hydrophobicity plot (Kyte-Doolittle, w = 9) (30) for the six MscS homologs in Escherichia coli. Blocks of sequence are highlighted as follows: periplasmic regions, green; membrane regions, gray; cytoplasmic domains, orange. Note that YbdG has a larger cytoplasmic domain than the other homologs due to an ~50-amino-acid insertion. (c) Comparison of the pore sequences between the six E. coli homologs. 1The protein sequences were aligned using ClustalW (72) and are depicted here for the sequence from residue 93 to residue 113 (MscS_E.coli). Residues shown in red are conserved with respect to the Gly-Ala pattern observed in TM3a of MscS from E. coli. Residues shown in blue are conserved either in terms of identity or character relative to the two Leu sealing rings (L105 and L109) from TM3a of MscS from E. coli. The Ala in YbdG (boxed) at the position equivalent to the upper-ring Leu in MscS (L105) has been confirmed by mutagenesis and confers a gain-of-function mutation in the absence of other inhibitory residues in TM3a that counter the effect of an Ala residue at the seal position (M.D. Edwards, U. Schumann & I.R. Booth, unpublished data). Note that position 113 (see text) is not conserved across the homologs. 2γ, conductance of the channel in nanoSiemens, measured under identical conditions. 3Unpublished data (M.D. Edwards, S.S. Black, S. Miller & I.R. Booth). 4Note that YbdG has not been measured in its native state; channel gating can be observed only after a mutation is introduced into the β-sheet domain (20). (d) Complimentary helix interfaces in MscS. The figure depicts TM3a for three subunits in ribbon format. The Gly and Ala residues that form the helix interface are depicted as dark gray and purple van der Waals spheres, respectively.

Europe PMC Funders Author Manuscripts

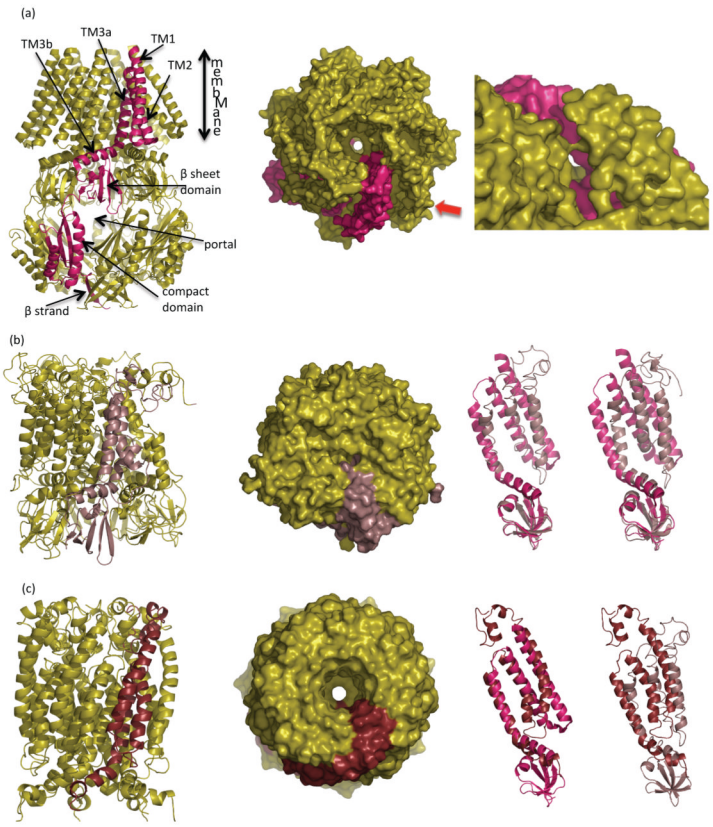

Fig 2.

Different experimental models for MscS in the closed form. (a, left) A ribbon diagram of the crystal structure MscS (9, 57). One subunit is shown in magenta. The key structural features discussed in the text are labeled. The cytoplasm is at the bottom; the periplasm is at the top. (a, right) Surface view of the MscS channel, looking downward from the periplasm to the cytoplasm. Two rings of Leu insert into the central cavity, creating a narrow hydrophobic pore. The crystal structure is asymmetric, and as a result the pore has an elliptical shape. (Inset) Viewed from the side it is clear that the TM helices are not tightly packed. There is a gap between TM2 and TM3a, allowing the neighboring TM2 (magenta) to be seen. This gap is also found in the open crystal structure and has been criticized as an artifact (5, 7, 11, 13). (b, i) The EPR-derived structure (65) after molecular modeling calculation (35). One subunit is colored pale pink. The model includes only the transmembrane helices and the β-sheet domain. (b, ii) The molecular surface showing a completely occluded pore, viewed downward from the periplasm to the cytoplasm. (b, iii) Superposition of one monomer of the original EPR model (pale pink) (65) with the closed crystal structure (magenta), the superposition is calculated using the β-sheet domain. The additional N-terminal region not seen in the crystal structure is visible. TM3a is little changed but TM1 and TM2 are different.

(b, iv) Superposition of the most divergent of the two calculated models (35) (pale pink) with the closed crystal structure (magenta). The superposition is calculated using the cytoplasmic domain. There is a more pronounced difference in TM3a, as well as in TM1 and TM2, with this model. (c, i) The extrapolated molecular dynamics model of the closed state of MscS (S. Sukharev, personal communication) (3). The model includes only the TM helices and a portion of the β-domain. One subunit is colored maroon. (c, ii) The molecular surface, with the closed and symmetrical pore, viewed downward from the periplasm to the

cytoplasm. The diameter of the pore is similar to the narrow diameter of the ellipse in the crystal structure but smaller than the long axis of the ellipse in the crystal structure. (c, iii) Superposition of one monomer of the extrapolated model (maroon) with the closed crystal structure (magenta). The superposition is calculated using residues 101 to 113 (TM3a). The additional N-terminal region not seen in the crystal structure is visible. There are pronounced differences in TM2. The kink at G113 is reduced and an additional kink at G121 is introduced. (c, iv) Superposition of one monomer of the extrapolated model (maroon) with the original EPR closed structure (pale pink). The N-terminal 27 residues (missing from the crystal structure) adopt a different structure in these two models. Abbreviations: EPR, electron paramagnetic resonance; MscS, mechanosensitive channel of small conductance; TM, transmembrane.

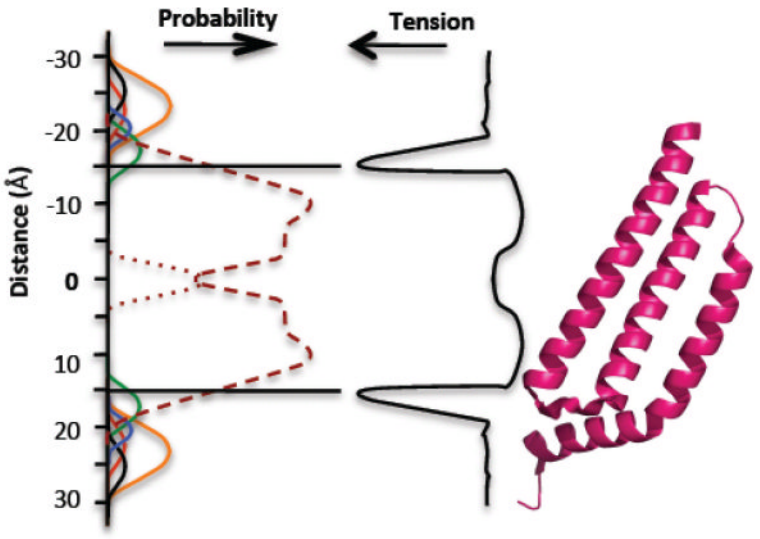

Fig 3.

The membrane bilayer and its relationship to MscS. (Left) The probability of different components of the phospholipid molecules occurring at positions relative to the center of the bilayer (50, 51): choline, black; phosphate, red; glycerol, blue; carbonyls, green; CH2 groups of fatty acids, purple dashed line; terminal CH3 groups of phospholipids, purple dotted line; water, orange line. (Center) Membrane tension (48, 49). (Right) A single subunit of MscS TM1, TM2, TM3a, and TM3b. Abbreviations: MscS, mechanosensitive channel of small conductance; TM, transmembrane.

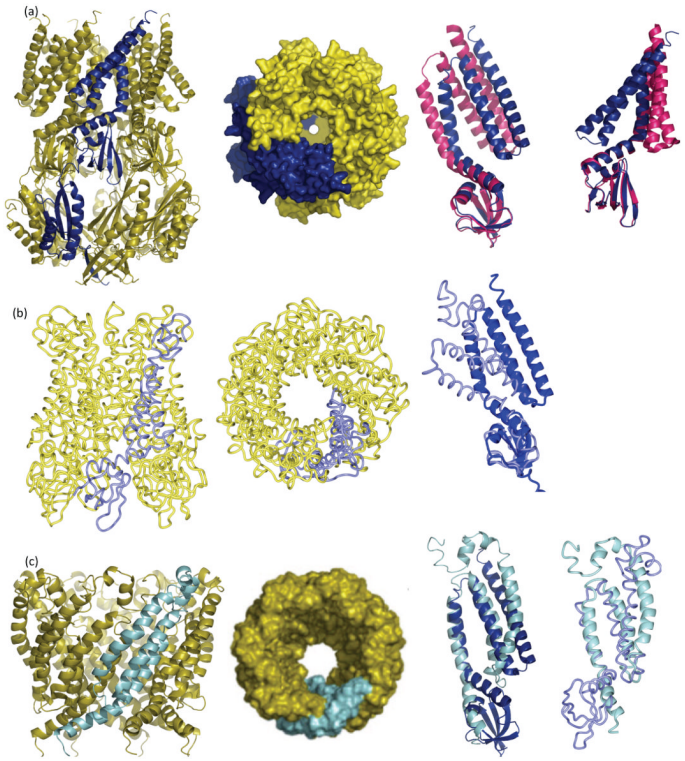

Fig 4.

Different experimental models for MscS in the open form. (a, i) A ribbon diagram of A106 MscS crystal structure. The A subunit (one of seven) is shown in blue (69). (a, ii) The surface representation, looking downward from the periplasm to the cytoplasm. The symmetrical pore opens to a diameter of ~14 Å . (a, iii) Superposition of one monomer of the A106V MscS (blue) with the closed crystal structure (magenta). The superposition is calculated using the β-sheet domain. (a, iv) Same as panel a, iv but in a different orientation. The movement of the TM1 and TM2 helices is pronounced. TM3a pivots at the kink at G113. (b, i) The EPR-derived open structure (66). Only cα coordinates are available, hence the different representation. The A subunit is colored pale blue. The model includes only the transmembrane helices and the β-sheet domain. (b, ii) The model viewed downward from periplasm to the cytoplasm. A surface cannot be calculated with cα coordinates only. (b, iii) Superposition of one monomer of the open EPR model (pale blue) with the A106V (open) crystal structure (blue). The superposition is calculated using the β-sheet domain. The additional N-terminal region not seen in the crystal structure is visible. The helices adopt a dramatically different orientation because the TM3a in the EPR structure undergoes a one-quarter rotation around its own axis, such that Leu105 (EPR model) superimposes with A106 (crystal structures).

(c, i) The extrapolated molecular dynamics model of the open state of MscS includes only the transmembrane helices and loops from the β-sheet domain (S. Sukharev, personal communication) (3). The A subunit is colored in cyan. (c, ii) The molecular surface of the open form has a diameter of 15.2 Å and a symmetrical pore. The diameter of the pore is slightly wider than the crystal structure.

(c, iii) Superposition of one monomer of the extrapolated model (cyan) with the open crystal structure (blue). The superposition is calculated using residues 101 to 113 (TM3a). In the extrapolated model, TM3 (TM3a + TM3b) is much longer and requires a change (currently not described) in the β-sheet domain as the extended helix interpenetrates within

the β-sheet domain. (c, iv) Superposition of one monomer of the extrapolated model (cyan) with the open EPR structure (pale blue). The superposition is calculated using residues 101 to 113 (TM3a) of extrapolated dynamics model and residues 102 to 114 of the EPR model. One residue shifts because TM3a in the EPR structure undergoes a one-quarter rotation around its axis (66). The N terminus, missing from the crystal structure, adopts different orientations in the two models as does TM1. The position of the β-sheet domain in the EPR model, like that observed in the crystal structure, is inconsistent with the extrapolated dynamics model. Abbreviations: EPR, electron paramagnetic resonance; MscS, mechanosensitive channel of small conductance; TM, transmembrane.